

## Johnson Thermo-Electrochemical Converter (JTEC) as a Heat to Electric Generator for Nuclear Power Systems

By: Dr. Lonnie G. Johnson<sup>1</sup>

<sup>1</sup>Johnson Research & Development, 263 Decatur St.; Atlanta, Ga., 30312; Ph: 404-584-2475

Future space Nuclear Power Systems (NPS) will include both Radioisotope Power Systems (RPS) and Fission Power Systems (FPS, Nuclear Reactors). The Johnson-Thermo-Electrochemical Converter (JTEC) is a solid state heat engine that has the potential for converting NPS heat into electricity at efficiency levels as high as 30 to 40% net, 70 to 80% of Carnot. Over the past five decades, conventional thermoelectric converters (Seebeck) have only achieved efficiency levels less than 15% of Carnot (6% to 8% net). As a more efficient replacement for existing thermoelectric technology, JTEC will provide NASA an attractive alternative for addressing the ever present need to minimize the amount of mass that must be delivered to space using expensive launch vehicles. A laboratory proof of concept demonstration has been successfully completed and an initial application analyses has been performed to understand the technology and its potential impacts at maturity. JTEC represents an opportunity to develop common technology that feeds both FPS and RPS and, thereby, support a full spectrum of requirements.

### I. The JTEC Description

JTEC uses an ionizable gas such as hydrogen or oxygen as a working fluid and Membrane Electrode Assemblies (MEA) to electrochemically convert heat into electricity. An MEA is comprised of an ion conductive membrane sandwiched between a pair of electrodes. Two MEA cells are coupled back to back to electrochemically perform the required heat engine working fluid compression and expansion processes, one operating at low temperature and the other at high temperature.

As illustrated in Figure 1a, the Membrane Electrode Assembly (MEA) cells used in the JTEC are similar to those used in fuel cells; but, there is only one ionizable gas and no water or other reaction product. If a MEA under an ionizable gas pressure differential is connected to an external load and current is allowed to flow, the gas on the high-pressure side will be oxidized

whereby its ion can be conducted through the ion conductive membrane as electrons are conducted through the external circuit. The pressure differential performs the work needed to produce electrical power. The ions and electrons are reduced back into gas at the membrane-electrode interface on the low pressure side. The process operates in reverse. Power can be applied to a MEA to pump gas from low pressure to high pressure.

The voltage of the MEA cell is defined by the Nernst<sup>1</sup> relationship as given in Equation 1, where  $V_{OC}$  is open circuit voltage,  $R$  is the universal gas constant,  $T$  is the cell temperature,  $F$  is Faraday's constant,  $P_H$  is the pressure on the high pressure side and  $P_L$  is the pressure on the low pressure side and the ratio is  $P_H/P_L$ . Note that the cell voltage is linear with temperature.

$$V_{OC} = \frac{RT}{2F} \ln\left(\frac{P_H}{P_L}\right) \quad \text{Equation 1}$$

Figure 1b shows an ideal temperature entropy diagram for the Ericsson thermodynamic cycle. The ideal Ericsson cycle is Carnot equivalent. Given the linear relationship between temperature and voltage,  $T_H$  has a corresponding  $V_H$  and  $T_L$  has a corresponding  $V_L$ .

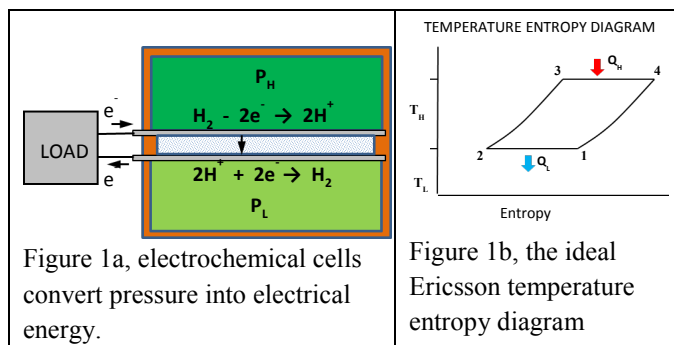


Figure 2, shows the JTEC thermodynamic process. Two cells are connected back to back with one MEA cell coupled to a high temp,  $T_H$ , heat source,  $Q_H$ , and the other coupled to a low temp,  $T_L$ , heat sink,  $Q_L$ . A recuperative heat exchanger (HX) connects high and low

pressure working fluid flow between the two cells. The indicated states 1 through 4 are identical at the respective points labeled in Figure 2 and the Ericsson cycle shown in Figure 1b. Beginning at low temperature-high pressure state 1, electrical energy  $P_{in}$  is supplied to the low temperature (low voltage) MEA to compress gas from low pressure state 1 to high pressure state 2. The temperature of the gas is maintained at low temperature by removing heat of compression  $Q_L$  from the ion conductive membrane (ICM) during the process. From state 2, the compressed gas passes through the recuperative, counter flow heat exchanger and is heated under essentially constant pressure to high temperature state 3. The heat needed to elevate the temperature of the gas from state 2 to 3 is transferred from gas flowing in the opposite direction through the heat exchanger. At high temperature, high-pressure state 3, electrical power  $P_{out}$  is generated by the high temperature (high voltage) MEA as gas expands from high pressure state 3 to low pressure state 4. Heat  $Q_H$  is supplied to the thin film ICM to maintain a near constant temperature expansion process. From state 4 to state 1, gas flows through the recuperative heat exchanger whereby its temperature is lowered at essentially constant pressure by heat transfer to gas passing from state 2 to 3. From state 1, the low pressure gas is recompressed through the low temp MEA from state 1 back to low-pressure state 2 as the cycle continues.

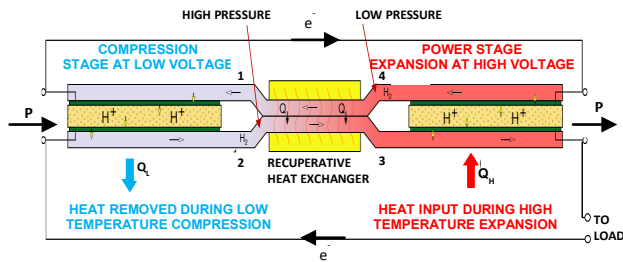


Figure 2, Functional Diagram of a JTEC heat to electric converter

## II. Status of JTEC technology

Figure 3 is a diagram of a JTEC used to perform a proof of concept demonstration. It was conducted using para-polybenzimidazole (pPBI) as the conducting polymer membranes and  $1.0 \text{ mg/cm}^2$  Pt loaded carbon based electrodes mounted in a polycarbonate housing structure. A pair of bi-polar high temperature MEA and a pair of bi-polar low temperature MEA are contained at opposite ends of the housing. The MEA share a common low pressure flow section which is defined by a pair of pPBI

membranes which extend the length of the unit. Operation was initiated by opening the purge ports and connecting a source of hydrogen the self-sealing input ports. Once flushed with hydrogen, the purge ports were plugged and the hydrogen source was disconnected. The coolant and heat source tubes were electrically connected to each other and used a common terminal for the low pressure electrodes. A power source was connected between the low pressure electrode terminals (coolant tubes) and the high pressure electrode terminals to pump hydrogen to the high pressure side to create a pressure differential.

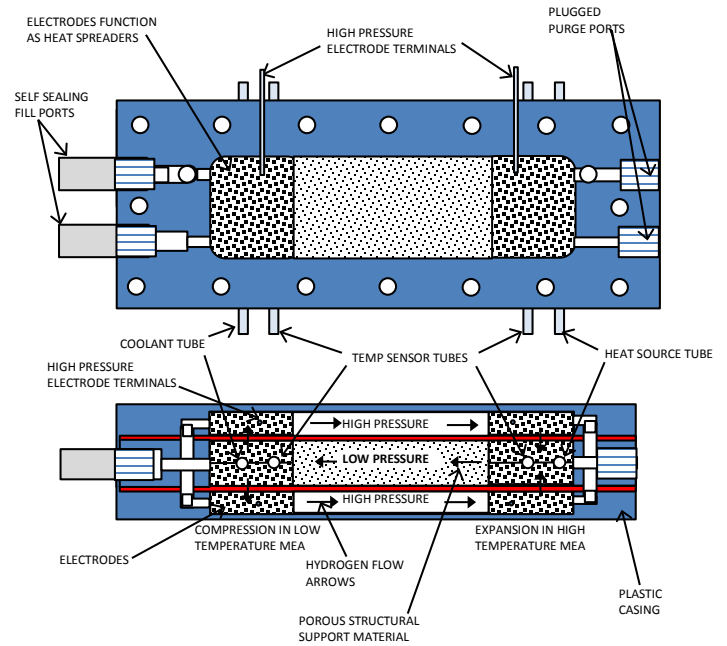


Figure 3, diagram of the demonstration unit.

The temperature of one MEA was then increased using a cartridge heater inserted in the heat source tube. This resulted in its temperature and voltage being higher than the temperature and voltage of the unheated MEA. Once a temperature differential was established, a 30 ohm resistive load was connected in series between the high and low temperature MEA as illustrated by the schematic diagram in Figure 4. The higher voltage of the heated MEA caused it to drive current against the voltage of the low temperature MEA. As hydrogen expanded from high pressure to low pressure through the high temperature MEA, its higher voltage forced reverse current through the low temperature MEA causing it to continuously pump hydrogen from low pressure to high pressure and thereby maintain a stable pressure

differential and thereby stable operation. A Hantek™ system was used to monitor current, voltage, and temperature. The high temperature MEA was maintained at 97.5°C and displayed an output voltage of 106.7 mVolts. The net output voltage difference between the high and low temperature MEA was 63.4 mVolts applied across the 30 Ohm load. The unit was operated for two hours and remained stable.

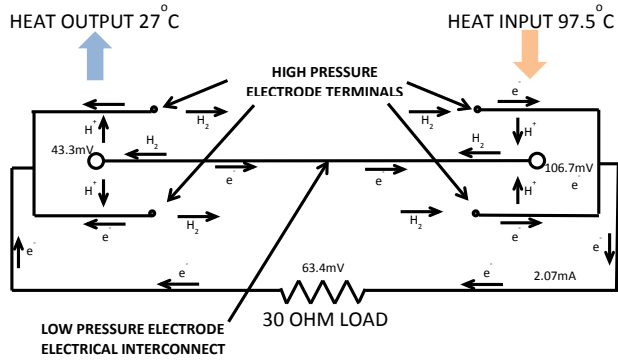


Figure 4, diagram showing the electrical connections of the JTEC supplying power across a 30 Ohm resistor

### III. JTEC Analytical Model

Figure 5 shows a computational model used to derive JTEC performance estimates. The high and low temperature membrane electrode assembly stacks are each modeled as voltage sources with internal impedance. The model computes MEA cell impedance to determine the resistance losses associated with ion conduction through the membranes based on conductivity of membrane materials, membrane thicknesses and efficiency losses associated with gas flow. MEA temperatures and the applied pressure ratio are used to calculate the open circuit voltage generated by the converter. The percentage of Carnot efficiency is equivalent to the percentage of the converter's open circuit voltage that is applied to the external load with current flow. When there is no current flow, the full open circuit voltage is output, the converter being Carnot equivalent only when there is no current flow and, thereby, no power output. Note that hydrogen is used as a working fluid in this example.

In operating the simulation model, a desired operating efficiency is chosen as a percentage of Carnot which yields a targeted output voltage as a percentage of

the open circuit voltage. The targeted portion of the open circuit voltage is applied to an external load. The remainder of the open circuit voltage is allocated to internal losses, including resistive losses and hydrogen flow losses. The portion allocated to resistive losses is used to determine the maximum level of current flow under which the voltage allocated to the external load can be maintained.

The calculation results in an initial current flow rate which defines the hydrogen flow rate. The portion of the voltage allocated to resistive losses is then modified considering the actual voltage of the high temperature MEA determined by the actual pressure ratio at the high temperature MEA calculated from pressure losses associated with hydrogen flow under the initial current. Next model applies the modified voltage across the MEA resistances to calculate the adjusted current level needed for the chosen percentage of Carnot. The flow rate is subsequently readjusted based on the results. The calculation is repeated for at least two iterations to determine a consistent current flow rate and level of hydrogen flow losses that result in the targeted voltage being applied to the load.

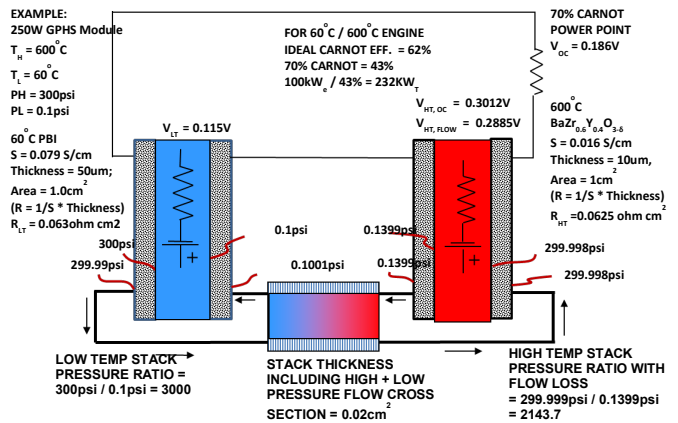


Figure 5, Computational model for a JTEC unit operating at a heat source temperature of 600°C and a sink temperature of 60°C.

Note that voltage loss due to hydrogen diffusion through the proton conductive membranes; voltage impact due to resistive heating of the high temperature MEA; and voltage loss due to recuperative heat exchanger effectiveness are presently being integrated into the modeling pending additional detailed heat exchanger

design parameters. Electrode conductivity and electrode/membrane interface impedance will be incorporated as a component of the membrane impedance.

The calculations are normalized to 1cm<sup>2</sup> for each MEA cell. The final step in the calculation is to scale the MEA area by an amount needed to achieve a targeted power level. In this example, the JTEC unit is scaled to an MEA total volume of 30cm<sup>3</sup> to operate on 62.5WT of heat input at a targeted efficiency of 70% of Carnot (43% net) to produce 100kWE of electrical output. The low temperature stack is operated at 600C and the high temperature stack at 600C. The pressure ratio is 3,000 with a low pressure of 0.1 psi and a high pressure of 300psi.

The high temperature MEA stack and the low temperature MEA stacks use different proton conductive membrane material based on stability and optimum ion conductivity over the targeted operating temperature ranges. Phosphoric acid doped Polybenzimidazole (PBI), a polymer material, is used for the low temperature stack. It demonstrates low molecular hydrogen diffusion and fast proton conductivity at low temperatures. On the other hand, Yttrium doped Barium Zirconate (Y<sub>0.2</sub>:BaZr<sub>0.8</sub>O<sub>3</sub>), a ceramic material, is used for the high temperature stack because of its conductivity in its operating temperature range and its high stability in pure hydrogen environments. The computations in Figure 8 are based on a PBI membrane thickness of 100μm and a ceramic membrane thickness of 10μm. The total hydrogen flow cross section is 200μm, 50μm high pressure flow cross section and 150μm for the low pressure flow cross section.

Note that although a pressure ratio of 3,000 is established within the engine by setting the pressure ratio of the low pressure stack and calculating its voltage, the pressure ratio at the high temperature stack is only 2143.7 due to drops in pressure due to friction losses as the hydrogen circulates within the engine, particularly on the low pressure side, yielding a concentration polarization effect. The lower pressure ratio at the high temperature stack results in a reduced voltage generated by the high temperature stack and, thereby, a loss in efficiency. Even with the losses incorporated to date, the performance projections remain impressive. The predicted power density is 0.79W/cm<sup>3</sup>.

#### IV. Implications for NASA

A monolithic co-sintered ceramic JTEC “chip” configuration appears attractive for space power generation. The notional conceptual configuration is shown in Figure 6. The approach is to use co-sintered proton conductive MEA structures based on an approach demonstrated by researchers at Georgia Tech, our

research partner. It shows a co-sintered MEA formed by porous ceramic electrodes sandwiching a non-porous ion conductive membrane. A co-sintering approach enables practical construction of high surface area MEA stacks having thin layers. Thin, high surface area membranes are important for minimizing internal resistance and thereby enabling high power density. The configuration is suitable for construction using 3-D printing or other suitable additive manufacturing techniques. Small, co-sintered JTEC chips will be formed having back-to-back MEA cells that are coupled to each other by a recuperative heat exchanger midsection. They will be configured for mounting within an exterior pressure vessel. Each chip has a bi-polar configuration with a common, internal low pressure section similar to that used for the proof-of-concept unit shown in Figure 3. The length of the assembly is 40mm with a width of 20mm. The total thickness including the electrode thicknesses and the flow cross sections is 0.520mm.

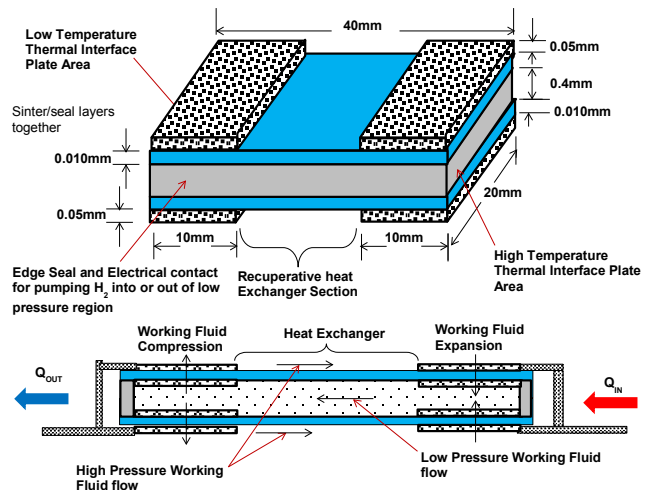


Figure 6, Co-sintered ceramic JTEC chip assembly

Figure 7 shows a concept for using JTEC chips to convert radioisotope heat into electrical power for future spacecraft. The heat source is located at the center of the housing with arrays of JTEC converter chips mounted along its sides. Heat spreaders couple the low temperature sides of the chips to the external housing. The external housing functions as a high pressure hydrogen containment reservoir and includes internal mounting supports to hold the chips in place and external radiator fins for heat dissipation. High pressure hydrogen flow between the high and low temperature ends of the JTEC occurs outside the chips but inside the pressure vessel. On the other hand, low pressure hydrogen occurs

inside the chips. Figure 8 illustrates the overall pressure containment structure.

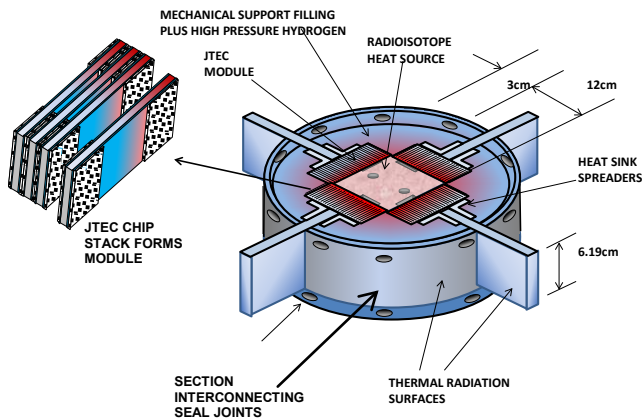


Figure 7, Notional concept for the use of JTEC chips to convert radioisotope heat into electrical power

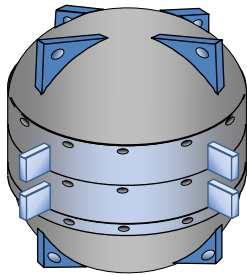


Figure 8, Notional concept of modular JTEC converter with overall pressure vessel.

## V. JTEC Implications for NASA

Table 1<sup>2</sup> was taken from the Radioisotope Power Systems Committee, National Research Council's report: "Radioisotope Power Systems: An Imperative for Maintaining U.S. Leadership in Space Exploration", ISBN 978-0-309-13857-4, 2009. It shows the performance of past, present, and future radioisotope power systems that are or have been under development by NASA. Conceptual implementations of a Radioisotope-powered Johnson Thermo-Electrochemical Converter (RJTEC) have been added to the chart for comparison purposes.

The projected conversion efficiency of the RJTEC is 40% operating on a 600°C heat source and a 100°C sink at 70% of Carnot. As illustrated in Table 1, the implication is that a RJTEC could produce 500 Watts of power, exceeding the ARTG's 430 Watts with its projected 15% conversion efficiency using only 5 GPHS

heat sources as opposed to the 12 required by the ARTG for the same electrical output. The reduction in power sub-system mass would be reduced from 40kg down to approximately 17kg, all else being equal. System design constraints would also be relaxed because of the dramatic reduction in waste heat that must be rejected from the spacecraft during launch and while in space. The ARTG 500 will have to reject over 2,500 watts of waste heat as opposed to only 750 watts of waste heat for the RJTEC.

	GPHS-RTG Past	MMRTG Present	ASRG Development	ARTG Future	TPV Future	40% RJTEC	40% RJTEC
Electric Output, BOM, W <sub>e</sub>	285	125	~140-150	~280-420	~38-50	500	300
Heat Input, BOM, W <sub>e</sub>	4500	2000	500	3000	250	1250	750
RPS System Weight, KG	6.3	6.3	~28-30	~9-14	~15-20	40	40
Total System Weight, kg	56	44.2	~19-21	~40	~7	~17	10
Specific Power, W <sub>e</sub> /kg	5.1	2.8	~7-8	~7-10	~6-7	~30	~30
Number of GPHS Modules	18	8	2	12	1	5	3
GPHS Module Weight, kg	25.7	12.9	3.2	19.3	1.6	8	4.8
<sup>238</sup> Pu Weight, kg	7.6	3.5	0.88	5.3	0.44	2.2	1.32

NOTE: ARTG, Advanced Radioisotope Thermal Generator; ASRG, Advanced Stirling Radioisotope Generator; BOM, Beginning Of Mission; GPHS, General Purpose Heat Source; MMRTG, Multi-Mission Radioisotope Thermoelectric Generator; RTG, radioisotope thermal generator; TPV, thermophotovoltaic.

Table 1, Performance of past, present, and future radioisotope power systems compared to two conceptual RJTEC configurations<sup>2</sup>.

Clearly, this technology has significant implications for NASA and warrants a significant, focused, development effort to determine its full potential.

## ACKNOWLEDGMENTS

Johnson Research and John Hopkins Applied Physics Laboratory are starting a collaboration project sponsored by the Radioisotope Power Systems Program to further explore the concept and advance JTEC technology.

## REFERENCES

1. J.H. Hirschenhofer, D.B. Stauffer, R.R. Engleman, and M.G. Klett, Fuel Cell Handbook, Fourth Edition, p. 2-5, 1999
2. "Radioisotope Power Systems: An Imperative for Maintaining U.S. Leadership in Space Exploration", ISBN 978-0-309-13857-4, 2009.